

Centrality dependence of freeze-out parameters from Au+Au collisions at $\sqrt{s_{NN}} = 7.7, 11.5$ and 39 GeV

Research Article

Lokesh Kumar* (for the STAR collaboration)

Kent State University, Kent, OH-44242, USA

Abstract: The RHIC beam energy scan program in its first phase collected data for Au+Au collisions at beam energies of 7.7, 11.5 and 39 GeV. The event statistics collected at these lower energies allow us to study the centrality dependence of various observables in detail, and compare to fixed-target experiments at SPS for similar beam energies. The chemical and kinetic freeze-out parameters can be extracted from the experimentally measured yields of identified hadrons within the framework of thermodynamical models. These then provide information about the system at the stages of the expansion where inelastic and elastic collisions of the constituents cease. We present the centrality dependence of freeze-out parameters for Au+Au collisions at midrapidity for $\sqrt{s_{NN}} = 7.7, 11.5,$ and 39 GeV from the STAR experiment. The chemical freeze-out conditions are obtained by comparing the measured particle ratios (involving $\pi, K, p,$ and \bar{p}) to those from the statistical thermal model calculations. The kinetic freeze-out conditions are extracted at these energies by simultaneously fitting the invariant yields of identified hadrons ($\pi, K,$ and p) using Blast Wave model calculations.

PACS (2008): 25.75.Nq, 25.75.-q, 25.75.DW, 12.38.Mh, 21.65.Qr

Keywords: beam energy scan • QCD phase diagram • critical point • transverse momentum spectra • chemical and kinetic freeze-out

© Versita Warsaw and Springer-Verlag Berlin Heidelberg.

1. Introduction

The experiments at the Relativistic Heavy-Ion Collider (RHIC) aim to look for the signatures of the production of a Quark-Gluon Plasma (QGP). The RHIC Beam Energy Scan (BES) [1] program is devoted to study the QCD phase diagram which involves searching for the QCD phase boundary and the QCD critical point [2]. The QCD phase diagram is usually represented by plotting temperature T vs. baryon chemical potential μ_B . There are two main phases expected in the QCD phase diagram - QGP and hadronic gas phase. The plan of the RHIC BES is to collect data at different center-of-mass energies and look for the possible signatures of a QGP and QCD critical point. It might then also be possible to locate the beam energy below which there is no QGP formation.

* E-mail: lokesh@rcf.rhic.bnl.gov

To access the phase diagram, one needs T and μ_B corresponding to the beam energy, which can be obtained from the spectra and ratios of produced particles.

The bulk properties of particle production in heavy-ion collisions can be studied using identified particle spectra. The measurements of particle abundances and transverse momentum distributions could provide information about the final stages of the collision evolution at chemical and kinetic freeze-out. The statistical thermal model [3] has successfully described the ratios of hadron yields produced in heavy-ion collisions from lower to higher energies. The centrality dependence of model parameters, especially at low energies could provide further understanding of the collision dynamics.

In this paper, we present the first measurements of centrality dependence of freeze-out parameters at $\sqrt{s_{NN}} = 7.7, 11.5$ and 39 GeV. The results are presented for midrapidity $|y| < 0.1$ region. The data are taken by the STAR experiment for Au+Au collisions in the year 2010. The total events analyzed are about 4 M, 8 M, and 10 M, respectively for $\sqrt{s_{NN}} = 7.7, 11.5,$ and 39 GeV. The centrality selection is done using the uncorrected charged track multiplicity measured event-wise in the TPC within $|\eta| < 0.5$. Centrality classes represent the fractions of this multiplicity distribution. The average numbers of participating nucleons $\langle N_{\text{part}} \rangle$ are obtained by comparing the multiplicity distribution with that from Glauber Monte simulation [1].

2. Results and Discussions

The transverse momentum spectra of hadrons (π , K , and p) are obtained for the Au+Au collisions at $\sqrt{s_{NN}} = 7.7, 11.5$ and 39 GeV and different centralities [4]. The proton spectra are not feed-down corrected for weak decays. The particle yields and ratios are used to obtain the freeze-out conditions. The statistical thermal model (THERMUS) [3] is used to extract the chemical freeze-out conditions at these energies. Kinetic freeze-out conditions are obtained by fitting the spectra with the Blast-Wave (BW) model calculations [5].

2.1. Chemical freeze-out

The scenario after the collisions when the inelastic collisions among the particles stop is called the chemical freeze-out. At this stage, the particle yields and ratios are finalized and do not change afterwards. The system can be described by the thermal equilibrium model (THERMUS). The model assumes thermal and chemical equilibrium. The main fit parameters are chemical freeze-out parameter T_{ch} , baryonic chemical potential μ_B , strangeness chemical potential μ_S , and strangeness suppression factor γ_s . The grand-canonical (GC) approach is used to fit the experimental particle ratios (π^-/π^+ , K^-/K^+ , \bar{p}/p , K^-/π^- , and \bar{p}/π^-). For GC ensemble, the baryon number, charge number, and strangeness content are conserved on average. The model explains the data very well.

Figure 1 shows the centrality dependence of chemical freeze-out temperature (left panel) and baryonic chemical potential (right panel). The T_{ch} increases with increasing energy. It also shows a slight increase as we go from

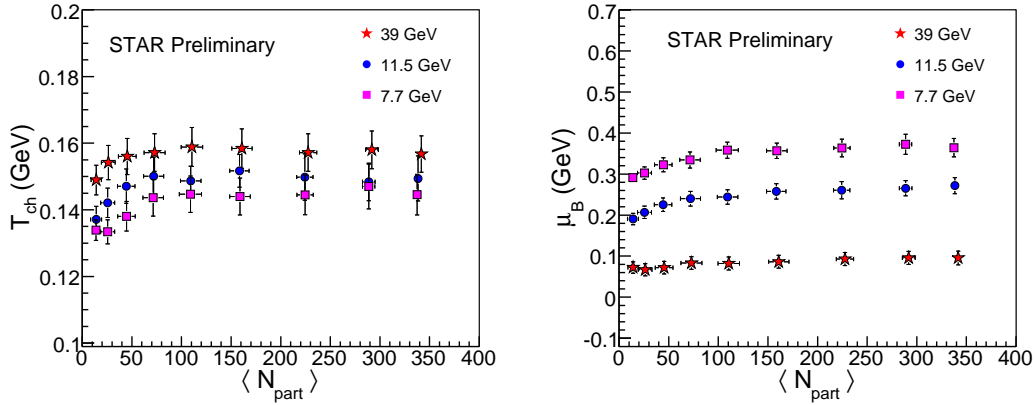


Figure 1. Left: T_{ch} as function of $\langle N_{\text{part}} \rangle$ for $\sqrt{s_{NN}} = 7.7, 11.5$ and 39 GeV. Right: μ_B as function of $\langle N_{\text{part}} \rangle$ for $\sqrt{s_{NN}} = 7.7, 11.5$ and 39 GeV. Errors represent the statistical and systematic errors added in quadrature.

peripheral to central collisions for all energies. The baryonic chemical potential increases with decreasing energy. This is because of large baryon stopping at mid-rapidity at low energies. The μ_B also shows a slight increase from peripheral to central collisions for these energies.

Figure 2 (left panel) shows the T_{ch} vs. μ_B plot. Results are shown for Au+Au collisions at $\sqrt{s_{NN}} = 7.7, 11.5, 39$ GeV and 200 GeV for different centralities. We see that the 200 GeV data do not show any centrality dependence for T_{ch} and μ_B . The 39 GeV data show a slight dependence of freeze-out parameters on centrality. However, when we go towards lower energies (11.5 and 7.7 GeV), we observe a clear centrality dependence of the T_{ch} and μ_B . This is the first observation of this behavior by any experiment. It may be noted that the freeze-out parameters shown here are obtained only from the ratios involving π, K, p and \bar{p} . It will be interesting to see the behavior of these parameters after including more ratios involving strange particles such as Λ and K_s^0 in THERMUS fits.

2.2. Kinetic freeze-out

Kinetic freeze-out represents the scenario when the interactions among the particles cease. After this time, the spectral shapes of the particle species do not change. The kinetic freeze-out conditions are obtained by fitting simultaneously the π, K, p spectra with the Blast-Wave model calculations. The BW model describes the spectral shapes assuming a locally thermalized source with a common transverse flow velocity field. The main fit parameters are the kinetic freeze-out parameter T_{kin} , the average flow velocity $\langle \beta \rangle$, and the velocity profile n . The right panel of Fig. 2 shows the variation of kinetic freeze-out temperature as a function of average flow velocity. Results are shown for different energies ($7.7, 11.5, 39, 62.4$ and 200 GeV) and for different centralities. T_{kin} decreases with increase in energy. It also decreases as we go from peripheral to central collisions. The $\langle \beta \rangle$ increases with increase in energy as well as collision centrality. The figure suggests that the higher value of T_{kin} corresponds to the lower value of $\langle \beta \rangle$ and vice-versa.

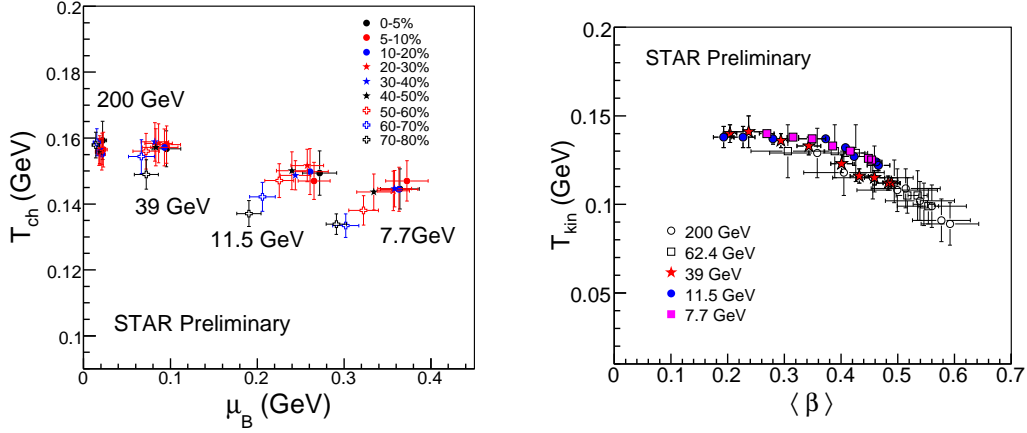


Figure 2. Left: Variation of T_{ch} with μ_B for different centralities at $\sqrt{s_{NN}} = 7.7, 11.5, 39$ and 200 GeV. Right: Variation of T_{kin} with $\langle \beta \rangle$ for different centralities at $\sqrt{s_{NN}} = 7.7, 11.5, 39, 62.4$ and 200 GeV. The 62.4 and 200 GeV results are taken from the Ref.[6]. Errors represent the statistical and systematic errors added in quadrature.

3. Summary

In summary, the centrality dependence of freeze-out parameters (kinetic and chemical) are presented for the BES energies 7.7, 11.5 and 39 GeV. The chemical freeze-out conditions are obtained using the particle ratios. For the first time, a clear centrality dependence of freeze-out parameters is observed at low energies. New measurements have extended the μ_B range covered by the RHIC data from 20-400 MeV in the QCD phase diagram. The kinetic freeze-out conditions are obtained by using the particle p_T spectra. The kinetic freeze-out temperature decreases with increase in energy and centrality. Average flow velocity increases with increase in energy and centrality.

We acknowledge the support from DOE and DAE-BRNS project sanction No. 2010/21/15-BRNS/2026.

References

- [1] B. I. Abelev *et al.* (STAR Collaboration), Phys. Rev. C **81**, 024911 (2010); STAR Internal Note-SN0493, 2009; arXiv:1007.2613; L. Kumar (STAR Collaboration), Nucl. Phys. A **830**, 275C (2009); *ibid* **862**, 125 (2011); B. Mohanty, Nucl. Phys. A **830**, 899C (2009).
- [2] Y. Aoki *et al.*, Nature **443**, 675 (2006); S. Gupta *et al.*, Science **332**, 1525 (2011); S. Ejiri, Phys. Rev. D **78**, 074507 (2008); E. S. Bowman and J. I. Kapusta, Phys. Rev. C **79**, 015202 (2009).
- [3] J. Adams *et al.* (STAR Collaboration), Nucl. Phys. A **757**, 102 (2005); P. Braun-Munzinger *et al.*, Phys. Lett. B **344**, 43 (1995); J. Cleymans *et al.*, Computer Physics Communications, **180**, 84 (2009).
- [4] L. Kumar (STAR collaboration), J. Phys. G: Nucl. Part. Phys. **38**, 124145 (2011).
- [5] E. Schnedermann *et al.*, Phys. Rev. C **48**, 2462 (1993).
- [6] B. I. Abelev *et al.* (STAR Collaboration), Phys. Rev. C **79**, 034909 (2009).